Modeling the Fluid-Wall Interaction in a Blood Vessel

G. PONTRELLI
Istituto per le Applicazioni del Calcolo – CNR, Rome, Italy

Summary

A differential model of blood flow through a compliant vessel is presented. A nonlinear, viscoelastic, constitutive equation for the wall is coupled with the one-dimensional, averaged fluid momentum equation. To describe wave propagation disturbances due to prosthetic implantations, the effects of changes in elasticity properties along the vessel are also studied. The nonlinear equation is solved by using the finite difference method on a staggered grid; some numerical simulations are then analyzed and discussed.

Key Words

Stent, wall-fluid interaction, viscoelasticity, hemodynamics

Introduction

Model studies of flows in liquid-filled, distensible tubes are conducted in order to understand the many aspects of the cardiovascular system in physiological and pathological states. Blood flow in arteries is dominated by instability and by wave-propagation phenomena generated by the interaction of the blood with the arterial wall. The importance of the arterial mechanics is widely recognized in modeling hemodynamic problems. Some work has been carried out with the simplistic assumption that the vessel wall is linearly elastic and isotropic [1,2]. Actually, the complex nature of biological tissues requires the development of nonlinear theories. Nonlinearities are not very relevant for predictions of wave speed, but do influence the pressure and flow-waveforms. This type of nonlinearity is a consequence of the curvature of the strain-stress function showing that an artery becomes stiffer as the distending pressure is raised. Some authors have shown that elasticity dominates the nonlinear mechanical properties of arterial tissues, whereas the vessel viscosity can be considered as a second-order effect [3]. On the other hand, experimental studies indicate that the arterial material is viscoelastic and anisotropic [4]. In principle, the viscoelastic dissipation of the vascular wall proves to be more important than the viscous dissipation of the blood. In fact, the latter can be neglected in a number of applications involving large blood vessels [1]. A review of the theoretical developments and new trends in arterial mechanics is given in [5].

Many theoretical and experimental formulations have been developed to describe the finite deformation and the nonlinear viscoelasticity of arteries in time-dependent flows. A nonlinear constitutive relation for the vascular wall that depends on the Green strains has been introduced in [6] and a stability analysis of the saccular aneurysm evolution is presented in [7]. In the present work, such a model is expanded to include the effects of the viscoelasticity of the solid wall. This is done in the following by letting the stress be a function

of both the strain and the strain rate. The inertia of the wall mass, even including the effective mass from the surrounding soft tissues, is negligible compared with the elastic force because of low wall velocities [1], and has been ignored.

Since we are interested in the pulse propagation phenomena, assuming a quasi-1D flow is a valid approach under the hypothesis that the wave amplitude is small and the wavelength long compared with the tube radius, so that the slope for the deformed wall remains small at all times [8]. A homogeneous nonlinear viscoelastic tube filled with an incompressible fluid was considered. All the quantities were assumed to vary in the axial direction, while the equations were averaged over the cross-section. The mathematical formulation of the problem and some numerical results are presented in the following for the unsteady flow sustained by pure oscillatory forcing, as a benchmark case. The flow dependence on the elasticity parameter and the mean pressure is shown. The effect of the elasticity parameter is related to the frequency of oscillations in the transient period, while the influence of viscosity parameter is to attenuate the natural oscillations, to reduce the tendency of shock formation as in a purely elastic wall model, and to counterbalance possible instability phenomena. Despite the nonlinearity of the elastic component, the results are qualitatively similar to those obtained with a linear elastic relation studied in [9], because of the small arterial deformations. Finally, the effect of a varying elasticity coefficient (e.g., due to a stent insertion [10,11]) on the flow dynamics is described.

However, the numerical value of the elastic and viscous coefficients appearing in the constitutive equation are critical and need to be carefully assessed by comparing numerical results with experimental measurements. Our aim is to achieve a satisfactory understanding of the mechanism of propagation of the pressure pulse, and of the changes in the pressure waveform which occur as a result of the nonlinear wall-fluid interaction as the pulse travels along the arteries.

Mathematical Models

The Viscoelasticity of the Vessel Wall

The adequate mechanical characterization of blood vessels is an important prerequisite for a quantitative description of blood flow, mostly in wave propagation phenomena. For an incompressible hyperelastic material, it is possible to define a strain-energy function W as a function of the stretch-ratio in variants I_1, I_2, I_3: this represents the elastically stored energy per unit volume in terms of the strain variables and represents a potential for the stress [12]. The problem of determining the form of the strain-energy function for biological materials has been examined from theoretical and experimental point of view. A variety of mathematical expressions for W has been proposed in biomechanics, depending on different materials and organic tissues; their efficiency is tested by their ability to match the experimental data over a wide range of strain values. As pointed out by Fung [4] and other authors [5], the properties of vascular tissues are highly nonlinear. Some attempts to define a non-linear strain-energy density function for the arterial tissue have been based on the static relationship between strains and elastic energy (see, for example, [4,6,13] and references therein).

Let us now consider the vessel wall modeled as an elastic axisymmetric membrane. This is a two-dimensional thin shell with a negligible mass compared with that of the fluid contained in it. The membrane is capable of deforming under the forces exerted by the fluid, is subject only to stresses in the tangential plane, and has no bending stiffness. Let $x_P(s)$, $r_P(s)$ be the Lagrangian coordinates of a particle P, with s being a parametric coordinate along the membrane in its symmetry plane. The strain-energy density function per unit area can be formulated as:

$$w = w(\lambda_1, \lambda_2) \tag{1.0}$$

where

$$\lambda_1 = \sqrt{\left(\frac{dr_p}{ds}\right)^2 + \left(\frac{dx_p}{ds}\right)^2} \qquad \lambda_2 = \frac{r_p}{R_u} \tag{1.1}$$

are the principal deformation ratios in the meridional and circumferential directions, and R_u is the undeformed radius. In this context, a constitutive strain-energy function modeling the mechanical properties of the arterial wall has recently been proposed [6,7] as:

$$w = c_0\left(e^Q - 1\right) \qquad Q = c_1\left(E_1^2 + E_2^2\right) + 2c_3E_1E_2 \tag{1.2}$$

where c_0 is a material parameter having the same dimensions as w (force/length), c_1 and c_3 are nondi-

mensional constants, and $E_k=(l^2_k-1)/2$; k=1,2 are the principal Green strains. Once the form of w is specified, the mechanical properties are completely determined, being the stress components (averaged across the thickness) along the longitudinal and circumferential directions given by differentiation of w:

$$T_1(\lambda_1,\lambda_2)=\frac{\lambda_1}{\lambda_2}\frac{\partial w}{\partial E_1}=\frac{1}{\lambda_2}\frac{\partial w}{\partial \lambda_1}$$

$$T_2(\lambda_1,\lambda_2)=\frac{\lambda_2}{\lambda_1}\frac{\partial w}{\partial E_2}=\frac{1}{\lambda_1}\frac{\partial w}{\partial \lambda_2} \qquad (1.3)$$

The former relations hold in the case of an incompressible and isotropic material, where principal directions of strain and stress coincide and express the property that the instantaneous Young's modulus increases with the strain, but with a different amount in the two directions [5]. Note that c_0 acts as a scaling factor for T_1 and T_2 (Figure 1). On the other hand, many authors have pointed out that the vessel walls are viscoelastic. Patel and Vaishnav verified the existence of arterial viscoelasticity through a dynamical experiment [8]. Reuderink found that neglecting the viscoelasticity causes an underestimation of both phase velocity and damping [2]. Generally, a viscoelastic wall model yields numerical results closer to physiological measurement than an elastic one, and a dissipative wall is

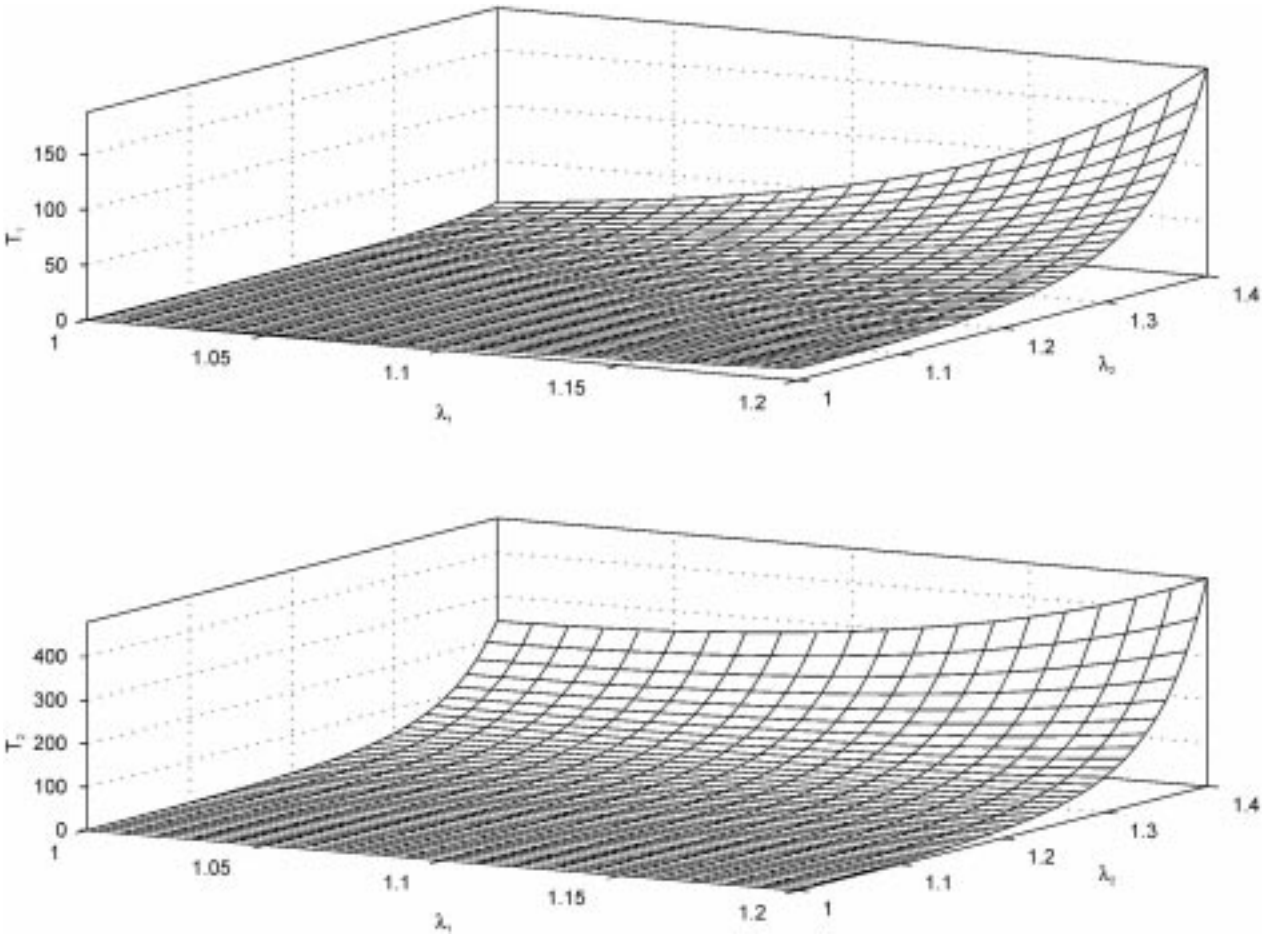

Figure 1. The strain-stress functions from Equation 1.3 with $c_0 = 1$, $c_1 = 11.82$, $c_3 = 1.18$. Definition of nondimensional elasticity coefficient c_0 is given in 2.0.

more effective than a dissipative fluid in eliminating the high frequency oscillations. The damping caused by viscoelasticity inhibits sharp peaks of the pressure and flow pulses and leads to more realistic results when compared with the experimental data [3]. The simplest generalization of (Equation 2.3) including a viscoelastic effect, is given the following strain-stress relationship:

$$T_1\left(\lambda_1,\lambda_2,\dot{\lambda}_1,\dot{\lambda}_2\right)=\frac{1}{\lambda_2}\frac{\partial w}{\partial \lambda_1}+\gamma\left(\dot{\lambda}_1+\frac{\dot{\lambda}_2}{2}\right)$$
$$T_2\left(\lambda_1,\lambda_2,\dot{\lambda}_1,\dot{\lambda}_2\right)=\frac{1}{\lambda_1}\frac{\partial w}{\partial \lambda_2}+\gamma\left(\dot{\lambda}_2+\frac{\dot{\lambda}_1}{2}\right) \qquad (1.4)$$

where $\gamma > 0$ is a wall viscosity coefficient and the dot denotes time derivative [14]. Although the inertia of the membrane is neglected and a general theoretical framework is still lacking, in the model case studied here, the simple functional dependence between strain and stress in Equations 1.4 takes into account the viscous effects of a material in time-dependent motions and models the response of the arterial wall to the deformation and to the rate of deformation. In other words, the Equations 1.4 mean that the membrane does not respond instantaneously to forces, as does a purely elastic body, but rather with a dissipative mechanism as a viscoelastic material.

The Wall-Fluid Coupling

Owing to the small deformations of the vascular wall and to the unidirectional nature of waves in the arterial tree, a quasi-one-dimensional model is adopted. Let us consider a homogeneous fluid of density r flowing in an axisymmetric distensible tube with a circular cross section, and let us introduce a set of nondimensional variables:

$$x\to\frac{x}{R_0}\qquad R\to\frac{R}{R_0}\qquad t\to\frac{tU_0}{R_0}$$
$$u\to\frac{u}{U_0}\qquad p\to\frac{p}{\rho U_0^2}\qquad c_0\to\frac{c_0}{\rho R_0 U_0^2} \qquad (2.0)$$

where x is the axial coordinate, R is the radius (with R_0 a reference constant radius), u is the axial velocity (with U_0 a characteristic velocity), p denotes the transmural pressure and t the time. Let us consider the 1D cross-averaged momentum equation:

$$\frac{\partial u}{\partial t}+u\frac{\partial u}{\partial x}=-\frac{\partial p}{\partial x}+f \qquad (2.1)$$

where f is a friction term [1]. This is approximated by the friction term of the Poiseuille steady flow in a tube of radius R given by:

$$f\approx-\frac{8u}{\mathrm{Re}\,R^2} \qquad (2.2)$$

with $\mathrm{Re}=U_0R_0/n$ the Reynolds number. As a consequence, the wall shear stress is approximated by:

$$\tau=\left.\frac{du}{dr}\right|_R\approx-\frac{4u}{\mathrm{Re}\,R} \qquad (2.3)$$

In principle, the former expressions (Equation 2.2 and Equation 2.3) hold for a steady flow in a rigid tube, but they are considered acceptable for quasi-steady flows and for small deformations $R \approx R_0$ [2]. In a deformable tube, the continuity equation is [1]:

$$\frac{\partial R}{\partial t}+\frac{R}{2}\frac{\partial u}{\partial x}+u\frac{\partial R}{\partial x}=0 \qquad (2.4)$$

Because of its small inertia, the vessel wall is modeled as a membrane which deforms under the fluid forces and reaches an equilibrium state. Let us indicate by R(x,t) and S(x,t) the Eulerian counterparts of the Lagrangian coordinates of a particle of the membrane (see previous section). The fluid-membrane equilibrium equations in tangential and normal directions are provided [12]:

$$R'(T_1-T_2)+RT_1'=\tau R\quad\left(1+R'^2\right)^{\frac{1}{2}}$$
$$\frac{-R''}{\left(1+R'^2\right)^{\frac{3}{2}}}T_1+\frac{1}{R\left(1+R'^2\right)^{\frac{1}{2}}}T_2=p \qquad (2.5)$$

where t is the shear stress exerted by the viscous fluid on the wall (Equation 2.3), nondimensional stresses T_1 and T_2 are defined as in Equation 1.4 and:

$$\lambda_1 = \sqrt{\frac{1+R'^2}{S'^2}} \qquad \lambda_2 = \frac{R}{R_0} \tag{2.6}$$

are the principal strains (the prime denotes x-derivative). The former Equations 2.1, 2.4, and 2.5 model the nonlinear fluid-wall interaction and are solved in the segment between the two points x = 0 and x = L which constitute the imaginary boundary of the differential problem. Since the flow is subcritical, a value for u (or p) has to be assigned at one boundary and a value for u (or p) at the other boundary. To understand the intrinsic fluid-wall dynamics, it is important to study the transient to the equilibrium configuration: in such a case, two constant values are assigned for p at the inlet and for u at the outlet:

$$p(0,t) = p_{ref} \qquad u(L,t) = u_{ref} \tag{2.7}$$

Alternatively, by considering the relevance of a pulsatile forcing in modeling vascular flows, two oscillatory boundary conditions are given at the extrema:

$$p(0,t) = p_{ref} + A_p \sin(2\pi S_t t)$$
$$u(L,t) = u_{ref} + A_u \sin(2\pi S_t t) \tag{2.8}$$

where A_p and A_u are nondimensional amplitudes and $S_t = R_0/(U_0T_0)$ is the Strouhal number and T_0 is the period of the incoming and outgoing waves. Since the arterial wavelength is much larger than the length of a vessel, the phase shift and difference in frequency at the inlet and outlet conditions (Equation 2.8) are small and do not significantly alter the dynamics of the system. Typical nondimensional values in physiological regimes are

$$u_{ref} = 0.5 \qquad A_u = 0.5 \qquad p_{ref} = 40$$
$$A_p = 10 \qquad S_t = 0.01 \tag{2.9}$$

for R_0 = 0.5 cm, U_0 = 50 cm/s, T_0 = 1 s and a mean pressure of 75 mmHg, respectively. Finally, the boundary conditions for S are imposed by considering an arbitrary value at x = 0 and a linear increasing at x = L, that is:

$$S(0,t) = 0 \qquad S'(L,t) = 1 \tag{2.10}$$

By evaluating the lower Equation 2.5 at the boundary points with the conditions R' = 0, R" = 0, two additional equations are obtained

$$pR = T_2 \tag{2.11}$$

which are equivalent to Laplace's law. The initial condition is chosen by considering an arbitrary configuration, which is obtained from the steady Poiseuille flow. Then the system is allowed to evolve toward its equilibrium configuration (Equation 2.7) or forced by an oscillating flow (Equation 2.8).

Numerical Methods and Results

The nonlinear equations describing the dynamics of the fluid-wall interaction are discretized using a second-order finite difference method centered in space. Let us consider a sequence of n+1 equidistant grid points x_i for i=0,...,n with $x_0 = 0$ and $x_n = L$. The spatial discretization is obtained by evaluating membrane stresses, strains, and their time derivatives (see Equations 1.4) at n inner points $x_i=(x_i+x_{i+1})/2$ of a staggered grid by considering averaged neighboring quantities. On the other hand, the equilibrium equations (Equation 2.5) and the fluid equations (Equations 2.1 – 2.4) are computed at the n-1 inner points x_i. The time discretization is based on the trapezoidal formula, in such a way the global scheme is of a second order in space and time. The resulting nonlinear system is solved by a globally convergent Newton type method. Nonlinear models turn out to be very sensitive to the many material parameters that characterize the specific flow problem. The reference values are fixed as c_1 = 11.82, c_2 = 1.18 [7], γ = 100 and u_{ref}, A_u, A_p and S_t as in 2.9. The other parameters have been chosen around some typical values to obtain results of physiological interest, and varied within a typical range to test the sensitivity of the system to perturbation. In particular, 5 £ c_0 £ 500 and 1 £ p_{ref} £ 200 was chosen. The values of c_0 and p_{ref} are not independent; since the deformation is proportional to the ratio p_{ref}/c_0, it turns out that for p_{ref}/c_0 ª < 0.01 the wall increases its stiffness and the numerical problem becomes harder. On the other hand, for a value of p_{ref}/c_0 that is too large, the system undergoes an unrealistically large deformation and the present model is not physically permissible.

In all the experiments, L = 8, $Dx = 10^{-2}$ and $Dt = 5 \times 10^{-4}$ were chosen. These values guarantee the numerical stability of the system for the set of parameters considered. The accuracy of the solution is controlled since the solution corresponding to a finer grid does not reveal a different structure or unresolved patterns. Since in wave propagation phenomena the dissipative effect of the blood viscosity is a minor effect [4], an inviscid fluid is considered (f = 0 in Equation 2.1 and $t = 0$ in upper Equation 2.5) in the following simulations.

Steady Case

For the equilibrium configuration (Equation 2.7), the effect of an arbitrary initial condition is irrelevant and dies out after a period of transience. After this initial transience all the variables asymptotically approach a steady-state value with damped oscillations (natural waves) exhibiting exponential decay and a c_0-dependent frequency S_t^* (natural frequency), computed by spectral analysis. Due to the the elasticity of the wall, a positive deformation R at the final state is found for $p > 0$. This steady deformation is independent of the wall-viscosity coefficient g and increases with the ratio p_{ref}/c_0. The natural waves disappear after a transient period depending on g, but numerical results show the existence of a critical value g_c below which spurious wiggles appear and difficulties in convergence arise. In this case the low viscosity of the wall is unable to attenuate the natural oscillations [15] and no stable steady solution has been found as $g \to 0$. A fundamental study of the natural waves in a viscoelastic tube and its dependence on the parameters has been carried out in [9].

Oscillatory Case

In the oscillatory case (Equation 2.8), the flow first interferes with the natural wave (see steady case, Equation 2.7) which, not being sustained, dies out in a short time. Afterwards the persistence of sinusoidal oscillations occurs with the same input frequency S_t over the mean values given in the steady case and with amplitudes depending on the elasticity parameter (see below), while the frequency of the wave does not change with c_0, p_{ref}, as does the natural frequency S_t^*. To avoid this effect caused by the initial conditions, in the numerical simulations the transient period has been dropped in the numerical simulations and only the solution after the second period is considered.

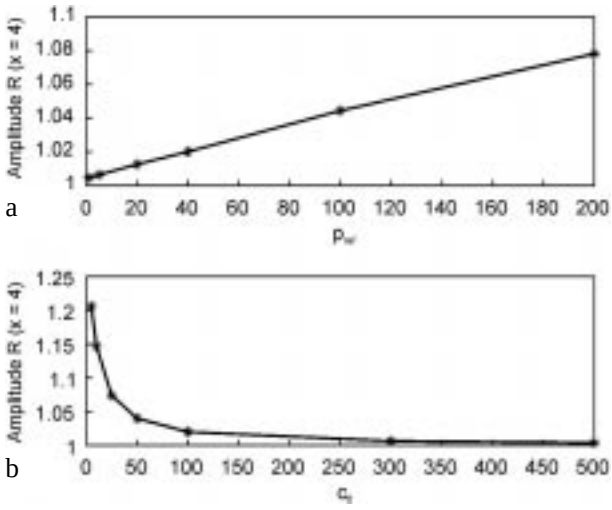

Figure 2. The deformation amplitude R (x = 4) (maximum value over time) at the center of the tube in panel a) for $c_0 = 100$ and varying mean pressure p_{ref} and in panel b) for $p_{ref} = 40$ and varying elasticity coefficient c_0. Starred points are results from simulations; continuous curves are obtained by a linear interpolation. See 2.0 and 2.9 for definition of nondimensional variables.

The value of the deformation is not influenced by g: the viscous damping affects only waves of relatively short length, such as those of the natural oscillation, but is irrelevant for pulses of long wavelength, such as those

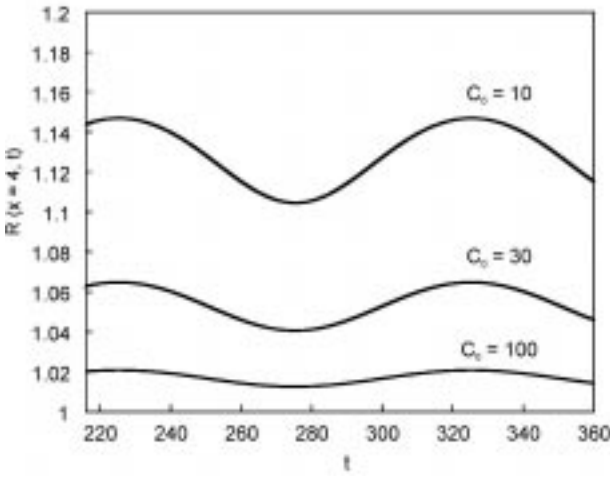

Figure 3. The time dependent deformation amplitude R (x = 4, t) at the center of the tube at x = 4 for three values of the elasticity coefficient c_0 for $p_{ref} = 40$. See 2.0 and 2.9 for definition of nondimensional variables.

in the vascular system ($S_t << S_t^*$). Nevertheless, a numerical instability is reported when $g \to 0$. The use of a numerical method devised for a purely elastic wall will be the subject of a future investigation. If not stated otherwise, the value $g = 100$ is considered in all the simulations. The longitudinal deformation S exhibits very small changes compared to the radial one and is not discussed.

As can be seen in Figure 2, the dependence of the amplitude of the deformation on p_{ref} is nearly linear, while that on c_0 is inversely linear. Figure 3 shows the evolution of R at the central point for three values of c_0. The analysis of the radial velocity proves that the propagation features correspond to transverse waves which do not propagate along the tube and are due to the boundary conditions that generate spurious reflections. The phenomenon is similar to that of a stretched string of a finite length with both ends oscillating. This drawback is overcome by coupling the present model with a lumped parameter model that accounts for the global circulation balance and induces travelling waves [16]. This will be done in a later study.

The present results agree qualitatively with those presented in [9] and show that the nonlinear character of the strain-stress function (see Equation 2.3) is responsible for minor changes with respect to the linear case. This is because of the small strains of the arterial motion; in the range of parameters considered: $\max_{xt} l_1 = 1.0003$ and $\max_{xt} l_2 = 1.2$.

Stent Insertion as a Clinical Application

The stenting methodology has been successfully employed for many years to treat many vascular pathologies that cause the arterial lumen to become extremely reduced. This method is based on the minimal invasive implantation of a tubular endoprosthesis, the stent, to support the arterial wall (Figure 4). Despite its complex geometrical structure and a variety of mechanical characteristics, a stent can be schematically represented as a stiff cylindrical sleeve placed in the vessel to prevent or correct narrowing of the section (stenosis) [10]. Although the stent implantation changes the geometry of the vessel and consequently induces significant disturbances in the local flow [11,17], the relevant effect in the wall-fluid interaction is the change of the compliance due to the sudden increase in the elasticity coefficient along the stent length.

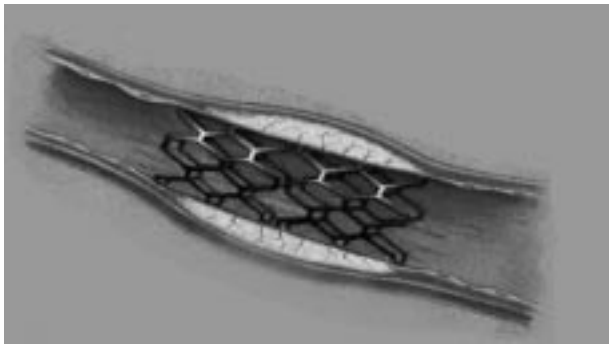

Figure 4. Implanted stent in a stenotic artery.

Let us consider a stent of length 2σ, centered on a point x^* and with an elasticity coefficient $c_s > c_0$. By considering the model from Equation 1.2, the elasticity parameter along the stented artery is given by

$$c(x) = \begin{cases} c_s & \text{if } |x - x^*| < \sigma \\ c_0 & \text{otherwise} \end{cases} \qquad (3.0)$$

However, to avoid a compliance mismatch between the relatively rigid stented segment and the distensible vessel, the elasticity coefficient is modeled by a continuous rapidly changing function (Figure 5):

$$c(x) = c_0 \left(1 + \delta\, e^{-\left(\frac{x - x^*}{\sigma}\right)^8} \right) \qquad \delta = \frac{c_s - c_0}{c_0} \qquad (3.1)$$

Thereby, for $c_s = c_0$, an uniform elasticity coefficient is recovered. The effect of a physiological local hardening or softening of an artery and the mechanical properties of stents can be also roughly modeled by varying the value of d and s.

In the numerical simulations, L = 8, x^*=4, s =2 (stent two diameters long), c_0 = 100 were fixed and d was varied up to 19 in Equation 3.1, with the wall viscosity coefficient g = 100 remaining constant. As expected, the maximum values of the deformation and the pressure at the center of the tube are reduced along with δ, and the asymptotic value of rigid wall is reached (Figure 6). On the other hand, the variation of the elasticity coefficient does not modify the frequency of the oscillation. The space-time evolution of the membrane radial velocity in a stented artery is depicted in Figure 7.

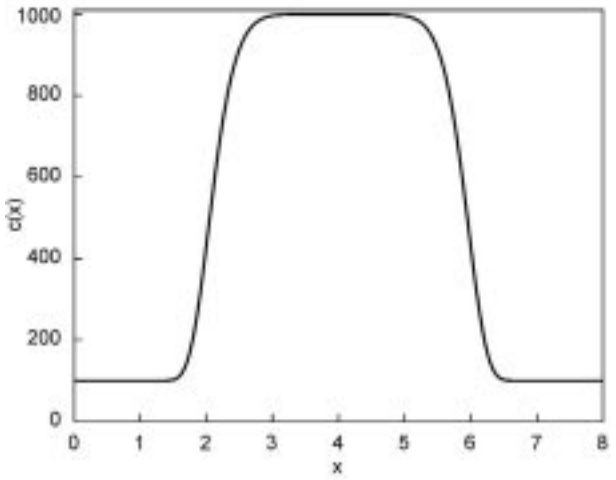

Figure 5. The elasticity function c(x) given by Equation 3.1 for $s = 2$, $x^* = 4$, $c_0 = 100$, $c_s = 1000$.

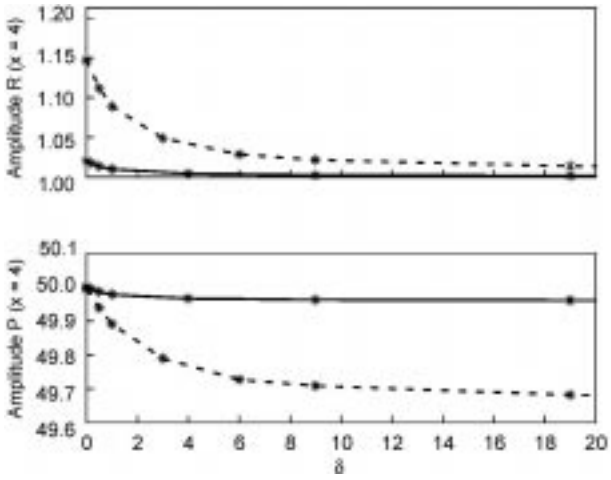

Figure 6. The deformation amplitude R (x = 4) pressure amplitude p (x =4) (maximum values over time) at the center of the tube and the center of the stented artery with d for $s = 2$ and $p_{ref} = 40$. Continuous line is for $c_0 = 100$, dashed line for $c_0 = 10$. See 2.0, 2.9 and 3.1 for definition of nondimensional variables.

Conclusion

The hemodynamics of the pulsatile flow in an arterial segment has been studied in relation to the viscoelastic properties of the vessel wall. The fluid-wall interaction is described by a one-dimensional model and is expressed by a set of four nonlinear partial differential equations. The dependence on the many parameters has been pointed out in the case of oscillatory flow, and the influence of some of these has been examined for a clinically relevant case. The issue of eliminating spurious reflections of the wave and of evaluating the wave speed needs to be addressed by assigning realistic pulsatile inflow and outflow conditions using a lumped parameter model. Finally, the geometrical, physical and biomechanical parameters need to be carefully identified with reference to a specific flow problem.

Acknowledgment

This work has been partially funded by the CNR Strategic Project: Mathematical Methods and Models for the Study of Biological Phenomena, 2000 (Progetto Strategico CNR: Metodi e modelli matematici nello studio dei fenomeni biologici, 2000).

References

[1] Pedley TJ. The fluid mechanics of large blood vessels. Cambridge: Cambridge University Press. 1980.

[2] Reuderink PJ , Hoogstraten HW, Sipkema P, et al. Linear and nonlinear one-dimensional model of pulse wave transmission at high Womersley numbers. J Biomech. 1989; 22: 819-827.

[3] Horsten JB, van Steenhoven AM, van Dongen AA. Linear propagation of pulsatile waves in viscoelastic tubes. J Biomech. 1989; 22: 477-484.

[4] Fung YC. Biomechanics: Mechanical properties of living tissues. 2nd edition. Berlin/New York: Springer Verlag. 1993.

[5] Humphrey JD. Mechanics of the arterial wall: Review and directions. Crit Rev Biomed Eng. 1995; 23: 1-162.

[6] Kyriacou SK, Humphrey JD. Influence of size, shape and properties on the mechanics of axisymmetric saccular aneurysms. J Biomech. 1996; 29: 1015-1022.

[7] Shah AD, Humphrey JD. Finite strain elastodynamics of intracranial saccular aneurysms. J Biomech. 1999; 32: 593-599.

[8] Patel DJ, Vaishnav RN. Basic hemodynamics and its role in disease processes. Baltimore: University Park Press. 1980.

[9] Pontrelli G. A mathematical model of flow through a viscoelastic tube. Istituto per le Applicazioni del Calcolo, CNR, Internal report 19. 1999.

[10] Xu XY, Collins MW. Flow pattern in stented arteries. Internal Medicine. 1997; 5: 29-32.

[11] Auricchio F, Di Loreto M, Sacco E. Finite-element analysis of a stenotic artery revascularization through a stent insertion. In: Middleton J, et al (editors). Computer Methods in Biomechanics and Biomedical Engineering, Volume 4. London: Gordon & Breach Publishing. In press 2001.

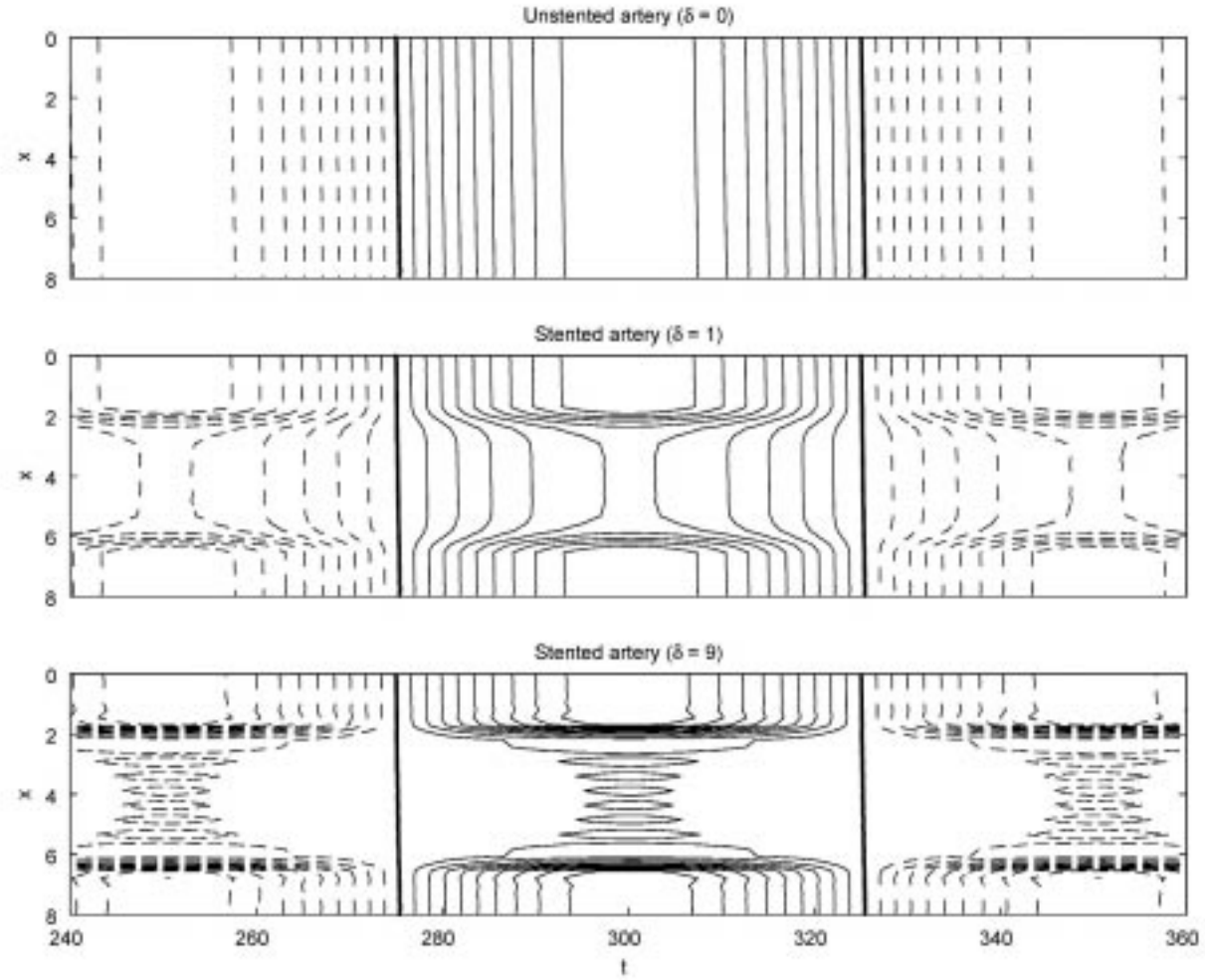

Figure 7. Space-time evolution of the membrane radial velocity in a stented artery with $c_0 = 100$, $s = 2$, and $p_{ref} = 40$ for $d = 0, 1, 9$. Thick line indicates the zero level, a continuous line denotes positive levels, and a dashed line denotes negative levels. See 2.0, 2.9 and 3.1 for definition of nondimensional variables.

[12] Green AE, Adkins JE. Large elastic deformations. Oxford: Clarendon Press. 1960.

[13] Demiray H. A quasi-linear constitutive relation for arterial wall material. J Biomech. 1996; 29: 1011-1014.

[14] Pedrizzetti G. Fluid flow in a tube with an elastic membrane insertion. J Fluid Mech. 1998; 375: 39-64.

[15] Pontrelli G. Nonlinear problems in arterial flows. Nonlinear Analysis: Theory, Methods and Applications. In Press 2001.

[16] Formaggia L, Nobile F, Quarteroni A, et al. Multiscale modelling of the circulatory system: A preliminary analysis. Comput Visual Sci. 1999; 2: 75-83.

[17] Peacock J, Hankins S, Jones T, et al. Flow instabilities induced by coronary artery stents: Assessment with an in vivo pulse duplicator. J Biomech. 1995; 28: 17-26.

Contact
Dr. Giuseppe Pontrelli
Istituto per le Applicazioni del Calcolo – CNR
Viale del Policlinico, 137
00161 Roma
Italy
Telephone: +39 06 88470251
Fax: +39 06 4404306
E-mail: pontrelli@iac.rm.cnr.it